REMARKS

The Examiner, Mr. Weatherby, is thanked for the courtesy extended applicants representatives during the interview of November 27, 2007, wherein, as noted in the Interview Summary, applicants provided a slide show providing descriptive details of the particulars of the invention, which features, as discussed generally at the interview, are now set forth in the newly submitted claims.

By the present amendment, claims 1 - 20 have been canceled without prejudice or disclaimer of the subject matter thereof and new claims 21 - 41 have been presented, wherein claims 21 and 37 are independent claims more particularly setting forth features of the present invention, as discussed below.

Applicants note that each of independent claims 21 and 37 are directed to an ultrasonic diagnostic apparatus as illustrated in Figs. 1 and 2 of the drawings of this application, which includes a tomographic image construction unit shown generally at 18 in combination with units 12, 14 and 16 in Fig. 1 for constructing gray scale tomographic images including a predetermined area of tissue of an object to be examined by repeatedly transmitting ultrasonic waves to the object at time intervals, and receiving time-series echo signals from the object including the predetermined area. Furthermore, an elasticity image construction unit represented generally by 20 in Fig. 1 is provided for constructing color elasticity images by measuring displacement of tissue of the object based on the time-series reflected echo signals which displacement is measured for example, by way of a pressure measuring unit 36, for example. In accordance with the present invention, an image composition unit is provided, as represented by 22 in Fig. 1, and as more clearly illustrated in Fig. 2, which generates composite images of the color elasticity image and the gray scale tomographic image including the predetermined area. Further, a display unit 24 is

provided for displaying a stiff area of the tissue of the object in the color elasticity image in relation to the predetermined area of the tissue of the object in the gray scale image so as to enable comparison of a spread condition of the stiff area of the tissue of the object in the color elasticity image with respect to the predetermined area of the tissue of the object in gray scale tomographic image whereby diagnosis of a condition of a tissue of the object is enabled. Applicants note that claim 37 further recites the features of an outline image construction unit described below.

As described in connect ion with Fig. 6 of the drawings of this application, for example, Fig. 6A illustrates a displayed monochrome or gray scale tomographic image which includes a tumor 60, and Fig. 6B displays a color elasticity outline image including a first border line 70 detected with a first threshold and a second border line 71 detected with a second threshold. Fig. 6C displays a combined or composite image of the gray scale or monochrome or tomographic image and the outline color elasticity image, wherein as shown in Fig. 6C, as described at page 17 of the specification, both border line 70 of the stiff region including tumor 60 and border line 71 of for example, a region 62 in which tissue is calcified are combined with the tomographic image in the display and by observing the image shown in Fig. 6C, the mutual relation between the tissue and the border line indicating elasticity behavior difference can be properly diagnosed. In this manner, since shape information obtained in the tomogrpahic image is emphasized in the display, the positional relation becomes more apparent and, for example, as described at page 17 of the specification, in cancer treatment, an expanse of the stiff region 61 with respect to an expanse and size of tumor 60 can be obviously grasped, and a removal region of the object can be properly determined. As an aid to the Examiner, submitted herewith is a copy of a publication of an article entitled "Breast Disease:

10

Clinical Application of US Elastography For Diagnosis by some of the inventors herein which appears in Radiology, Vol. 239, No. 2, May 2006, pages 341-350. As described at page 345 in the first full paragraph in the left hand column, "Image construction was performed by using a program developed by Hitachi Medical (T.M.)(9)", which is representative of the present invention. Applicants note that page 345 describes scoring to determine the possibility of cancer. Thus, as described in the specification of this application, with the present invention, an expanse of a stiff region with respect to expanse and size of tumor can be obviously grasped and a removal region of the object can be properly determined. That is, as now recited in the independent and the dependent claims of this application, a display unit displays a stiff area of the tissue of the object in the color elasticity image in relation to the predetermined area of the tissue of the object in the grasped tomographic image so as to enable composition of a spread condition of the stiff area of the tissue of the object in the color elasticity image with respect to the predetermined area of the tissue of the object in the gray scale tomographic image, whereby diagnosis of a condition of the tissue of the object is enabled.

As to the rejection of claims 1 - 3, 5 - 7, 13 and 16 - 19 under 35 USC 102(e) as being anticipated by Von Behren et al; the rejection of claims 4 and 20 under 35 USC 103(a) as being unpatentable over Von Behren et al in view of Sarvazyan; the rejection of claim 8 under 35 USC 103(a) as being unpatentable over Von Behren et al; the rejection of claims 9 and 10 under 35 USC 103(a) as being unpatentable over Von Behren et al in view of Sarvazyan; the rejection of claims 11 and 12 under 35 USC 103(a) as being unpatentable over Von Behren et al; and the rejection of claims 14 and 15 under 35 USC 103(a) as being unpatentable over Von Behren et al; such rejections are considered to be obviated by the cancellation of claims 1 - 20 and the

presentation of new claims 21 - 41. Further, applicants traverse the aforementioned rejections insofar as they are applicable to the newly submitted claims.

As to the requirements to support a rejection under 35 USC 102, reference is made to the decision of In re Robertson, 49 USPQ 2d 1949 (Fed. Cir. 1999), wherein the court pointed out that anticipation under 35 U.S.C. §102 requires that each and every element as set forth in the claim is found, either expressly or inherently described in a single prior art reference. As noted by the court, if the prior art reference does not expressly set forth a particular element of the claim, that reference still may anticipate if the element is "inherent" in its disclosure. To establish inherency, the extrinsic evidence "must make clear that the missing descriptive matter is necessarily present in the thing described in the reference, and that it would be so recognized by persons of ordinary skill." Moreover, the court pointed out that inherency, however, may not be established by probabilities or possibilities. The mere fact that a certain thing may result from a given set of circumstances is not sufficient.

Turning first to Von Behren et al, applicants submit that this patent merely indicates that an overlay display is preferably generated as a linear combination of a gray scale representation and a color representation. Irrespective of the contentions by the Examiner, applicants submit that Von Behren et al provides no disclosure or teaching of an image composition unit for generating composite images of the color elasticity image and the gray scale tomographic image including the predetermined area, and a display unit for displaying a stiff area of the tissue of the object in the color elasticity image in relation to the predetermined area of the tissue of the object in the gray scale tomographic image so as to enable comparison of a spread condition of the stiff area of the tissue of the object in the color elasticity image with

12

respect to the predetermined area of the tissue of the object in the gray scale tomographic image, whereby diagnosis of a condition of the tissue of the object is enabled. Applicants note that by applying the scoring based upon the comparison of the spread condition of the stiff area of the tissue of the object and the color elasticity image with respect to the predetermined area of the tissue of the object in the gray scale tomographic image, the diagnosis of a condition of the tissue of the object is enabled. In this manner, removal of a region of cancer can be properly determined. Applicants submit that Von Behren et al provides no disclosure or teaching of the recited features of independent claim 21 and claim 37, noting that claim 37 recites the additional feature of an outline image construction unit. Accordingly, applicants submit that independent claims 21 and 37 recite features not disclosed or taught by Von Behren et al in the sense of 35 USC 102 or 35 USC 103 such that all claims patentably distinguish thereover.

With respect to the secondary reference of Sarvazyan, applicants submit that while Sarvazyan teaches a pressure measuring unit, applicants note that Sarvazyan describes taking differences between two pressure profiles to obtain information on an inclusion as described with respect to Fig. 2 at column 6, lines 15 - 35 of such patent. However, Sarvazyan does not disclose an elasticity image construction unit including a pressure measuring unit for measuring information of pressure applied to the object in accordance with manual displacement of the tissue of the object for construction of a color elasticity image of the tissue of the object as recited in claim 29 and the dependent claims thereof, for example. Thus, Sarvazyan does not overcome the deficiencies of Von Behren et al in relation to the claimed invention and the proposed combination does not provide the claimed features as recited in the claims of this application. Furthermore, it is apparent that the cited art does not

13

provide an outline image construction unit operating in the manner defined and other features of the independent and dependent claims of this application as now recited. Accordingly, applicants submit that the independent and dependent claims patentably distinguish over Von Behren et al and Sarvazyan taken alone or in any combination thereof in the sense of 35 USC 103 and all claims should be considered allowable thereover.

In view of the above amendments and remarks, applicants submit that all claims present in this application should now be in condition for allowance and issuance of an action of favorable nature is courteously solicited.

To the extent necessary, applicants petition for an extension of time under 37 CFR 1.136. Please charge any shortage in the fees due in connection with the filing of this paper, including extension of time fees, to the deposit account of Antonelli, Terry, Stout & Kraus, LLP, Deposit Account No. 01-2135 (Case: 529.44847X00), and please credit any excess fees to such deposit account.

Respectfully submitted,

ANTONELLI, TERRY, STOUT & KRAUS, LLP

_____/Melvin Kraus/_____ _M_
Melvin Kraus
Registration No. 22,466

MK/jla
(703) 312-6600

14

Radiology

Breast Disease: Clinical Application of US Elastography for Diagnosis[1]

Ako Itoh, MD
Ei Ueno, MD, PhD
Eriko Tohno, MD, PhD
Hiroshi Kamma, MD, PhD
Hideto Takahashi, PhD
Tsuyoshi Shiina, PhD
Makoto Yamakawa, PhD
Takeshi Matsumura, MS

Purpose: To evaluate the diagnostic performance of real-time free-hand elastography by using the extended combined autocorrelation method (CAM) to differentiate benign from malignant breast lesions, with pathologic diagnosis as the reference standard.

Materials and Methods: This study was approved by the University of Tsukuba Human Subjects Institutional Review Board; all patients gave informed consent. Conventional ultrasonography (US) and real-time US elastography with CAM were performed in 111 women (mean age, 49.4 years; age range, 27–91 years) who had breast lesions (59 benign, 52 malignant). Elasticity images were assigned an elasticity score according to the degree and distribution of strain induced by light compression. The area under the curve and cutoff point, both of which were obtained by using a receiver operating characteristic curve analysis, were used to assess diagnostic performance. Mean scores were examined by using a Student t test. Sensitivity, specificity, and accuracy were compared by using the standard proportion difference test or the Δ-equivalent test.

Results: For elasticity score, the mean $\pm$ standard deviation was 4.2 ± 0.9 for malignant lesions and 2.1 ± 1.0 for benign lesions ($P < .001$). When a cutoff point of between 3 and 4 was used, elastography had 86.5% sensitivity, 89.8% specificity, and 88.3% accuracy. When a best cutoff point of between 4 and 5 was used, conventional US had 71.2% sensitivity, 96.6% specificity, and 84.7% accuracy. Elastography had higher sensitivity than conventional US ($P < .05$). By using equivalence bands for noninferiority or equivalence, it was shown that the specificity of elastography was not inferior to that of conventional US and that the accuracy of elastography was equivalent to that of conventional US.

Conclusion: For assessing breast lesions, US elastography with the proposed imaging classification, which was simple compared with that of the Breast Imaging Recording and Data System classification, had almost the same diagnostic performance as conventional US.

© RSNA, 2006

Generally, breast cancer tissue is harder than the adjacent normal breast tissue. This property serves as the basis for some examinations, such as palpation, that are currently being used in the clinical assessment of breast abnormalities, as well as for elastography.

The principle of elastography is that tissue compression produces strain (displacement) within the tissue and that the strain is smaller in harder tissue than in softer tissue. Therefore, by measuring the tissue strain induced by compression, we can estimate tissue hardness, which may be useful in diagnosing breast cancer.

Elastography has been used clinically to examine a variety of breast lesions in patients, and it has been concluded that this modality may be useful for differentiating malignant from benign masses (1).

During elastography, it is assumed that the main displacement of tissue occurs in the longitudinal direction (ie, in the direction of the beam). This condition can be largely met by applying compression with a well-controlled stepping motor. With freehand compression, however, the influence of probe movement on the skin's surface in the lateral direction (so-called creep or slip) must be suppressed. A high-speed algorithm for estimating strain distribution is required for real-time measurement. In addition, an ideal elastography system will have a large dynamic range of strain for stable measurements that does not depend on the speed and extent of compression.

Three methods—that is, the spatial correlation method, the phase-shift tracking method, and the combined autocorrelation method (CAM)—have been introduced for measuring tissue

strain at elastography. Although a head-to-head comparison of these methods is lacking, each method appears to have certain advantages and disadvantages (Table 1).

The spatial correlation method uses an ordinary two-dimensional pattern-matching algorithm to search for the position that maximizes the cross correlation between regions of interest (ROIs) that are selected from two images (one obtained before and the other obtained after deformation). This method can be used to demonstrate displacement in two dimensions (longitudinal and lateral), but the processing time is lengthy, which is a disadvantage for real-time assessment. The phase-shift tracking method is based on an autocorrelation method that is well known as a principle of color Doppler ultrasonography (US). As a result, this method can be used to rapidly and precisely determine longitudinal tissue motion because of phase-domain processing. Because of errors that are related to aliasing, the phase-shift tracking method fails when used to measure large displacements. In addition, this method poorly compensates for movement in the lateral direction, which is a disadvantage for freehand compression.

To overcome this problem, we developed a third method—the CAM (2–4). This method enables rapid and accurate detection of longitudinal displacement by using phase-domain processing without aliasing. Because lateral and elevational tissue movements are inevitable during palpation-like freehand manipulation of the probe, we modified the CAM to better demonstrate tissue displacement in these directions (5).

The dynamic range of strain that is estimated by using the extended CAM is 0.05%–5.00% (optimal dynamic range, 0.50%–2.00%); this method can com-

pensate for up to about 4 mm of lateral slip (5). We have further developed this system for clinical breast examination.

Thus, the purpose of our study was to evaluate the diagnostic performance of real-time freehand elastography by using the extended CAM to differentiate benign from malignant breast lesions, with pathologic diagnosis as the reference standard.

Materials and Methods

Patients

This study was approved by the University of Tsukuba Human Subjects Institutional Review Board, and all patients provided informed consent. All data collection, analysis, and information submitted for publication were controlled by authors who were not employees of Hitachi Medical, which provided the equipment used for this study. We performed real-time freehand US elastography in 135 consecutive women who underwent evaluation for breast lesions (76 benign lesions and 59 malignant lesions) at Tsukuba University Hospital between March 22, 2002, and September 26, 2003; lesions were detected at conventional B-mode US and were classified as category 2–5 lesions according to the Breast Imaging Recording and

Table 1				
Comparison of Different Methods for Measuring Strain				
Method	Processing Speed	Precision	Measureable Range of Strain	Sensitivity to Lateral Slip
Spatial correlation	Slow	Moderate	Large	Robust
Phase-shift tracking	Fast	High	Small	Weak
CAM	Fast	High	Large	Robust

Radiology

Data System (BI-RADS) criteria for US (6). Lesions were defined as areas in the breast tissue that were hypoechoic or isoechoic (compared with the subcutaneous fat) on B-mode images and included both mass-forming lesions and non–mass-forming lesions. At B-mode imaging, lesions that were clearly cystic or those that appeared as fat islands were not included.

Analyses were based on data from 111 patients in whom lesions measured no more than 30 mm in diameter and for whom cytologic or histologic diagnoses were obtained. Eight patients with lesions larger than 30 mm (one with a benign lesion and seven with malignant lesions) were excluded because these larger lesions could be diagnosed by using conventional diagnostic methods, such as cytology or biopsy. Furthermore, 16 patients (all with benign lesions) were excluded because no pathologic diagnosis was available. Overall, the remaining 111 patients had a mean age of 49.4 years (age range, 27–91 years). The 52 patients with breast cancer had a mean age of 52.9 years (age range, 29–91 years), and the 59 patients with benign lesions had a mean age of 47.4 years (age range, 27–73 years). This difference was not statistically significant according to the Welch test, which was used because pretest results (Bartlet test) did not show equal variance between groups. The diameter of malignant lesions (mean, 16.6 mm $\pm$ 6.1 [standard deviation]; range, 6–30 mm) was determined to be significantly greater than that of benign lesions (mean, 12.6 mm $\pm$ 6.2; range, 4–30 mm) by using the Student t test based on the pretest of variance equality (Bartlet test) ($P < .001$).

In all patients with benign or presumed benign lesions, we obtained follow-up data for a period of more than 1 year (ie, from the time of diagnosis to January 2005).

Pathologic Diagnoses

All diagnoses were made by a pathologist (H.K.) who had 20 years of experience in the pathologic analysis of breast cancer samples obtained with fine-needle aspiration cytology, needle biopsy,

excisional biopsy, or radical surgery, all of which were performed according to the established criteria (7,8). Lesions were first classified as malignant or benign. The most prevalent malignant lesions were further divided into three subgroups according to the criteria of Japanese Breast Cancer Society (7). These subgroups included ductal carcinoma in situ (DCIS), invasive ductal carcinoma of nonscirrhous type, and invasive ductal carcinoma of scirrhous type. Similarly, the most prevalent benign lesions were divided into three subgroups on the basis of histologic features; these subgroups included intraductal papilloma, fibroadenoma, and aberrations of normal development and involution (ANDI) without fibroadenoma (eg, duct papillomatosis, sclerosing adenosis, and lobular hyperplasia) (7,8).

Equipment

Conventional US was performed by using a digital electronic scanner with a frequency range of 9–13 MHz (HDI 5000; Philips Medical Systems, Bothell, Wash) and an annular-array mechanical sector scanner with a frequency of 7.5 MHz (SSA-250A; Toshiba Medical Systems, Tochigi, Japan). Color Doppler US was performed in a subset of patients by using a digital electronic scanner with a speed range of 3.5 cm/sec (HDI 5000; Philips Medical Systems). Examinations were performed by a surgeon (E.U.) who had 26 years of experience in breast US or by a radiologist (E.T.) who had 20 years of experience in breast US. All elasticity images were obtained with a system that consisted of a digital US scanner (EUB-6500; Hitachi Medical, Tokyo, Japan) that was remodeled exclusively for this study and an external personal computer (Dell, Round Rock, Tex); images were collected by a surgeon (A.I.) who had 5 years of experience in breast US. The US probe was a 7.5-MHz liner electronic probe (EUP-L53; Hitachi Medical) equipped with a handmade stabilizer that could press evenly against a wide area, thereby minimizing the creep and rotation of the probe on the skin's surface. None of the patients in

this study experienced adverse events from either conventional US or elastography.

Imaging Methods

Conventional US.—First, conventional US images of the breast were obtained. During our conventional examination, we obtained B-mode images first, and then color Doppler US was performed in patients with mass-forming lesions (104 of 111 lesions) to evaluate the vascularity of the mass, which was one of the BI-RADS criteria for US. Lesion size was defined as the diameter of the hypoechoic lesion at B-mode US.

Images were assigned to one of five categories according to the BI-RADS criteria for US (6): category 1, negative findings; category 2, benign findings; category 3, probably benign findings; category 4, findings suspicious for malignancy; and category 5, findings highly suggestive of malignancy.

Categories were assigned by either the surgeon (E.U.) or the radiologist (E.T.), both of whom were board certified by the Japanese Society of Ultrasonics in Medicine. These investigators determined the BI-RADS category of each lesion, with knowledge of the results of physical examination and mammography but without knowledge of the final pathologic diagnosis.

Elastography.—On the same day, we next obtained elasticity images as motion images, with the patient in the supine position and with the stabilizer-equipped probe oriented perpendicular to the chest wall. The probe was applied to the breast and was moved slightly inferior and superior to obtain the elasticity images.

Importantly, to obtain images that were appropriate for analysis, we applied the probe with only light pressure, which we defined as a level of pressure that maintained contact with the skin and permitted imaging conditions for which the association between pressure and strain was essentially proportional. We avoided using higher levels of pressure, which manifest nonlinear properties of tissue elasticity; in such circumstances, the association between pressure and strain is no longer proportional. It should be

noted, however, that the examiner did not have to maintain a specific level of pressure and that the dynamic range of pressure that was appropriate for elasticity images was wide enough to be controlled with freehand compression. Therefore, the examiner was able to gauge the proper pressure by monitoring the real-time elasticity image while mov-

ing the probe. Specifically, if pressure increased above a certain level, the pattern of the elasticity image started to change drastically as the pressure increased; therefore, we did not use images that were obtained above this level of pressure.
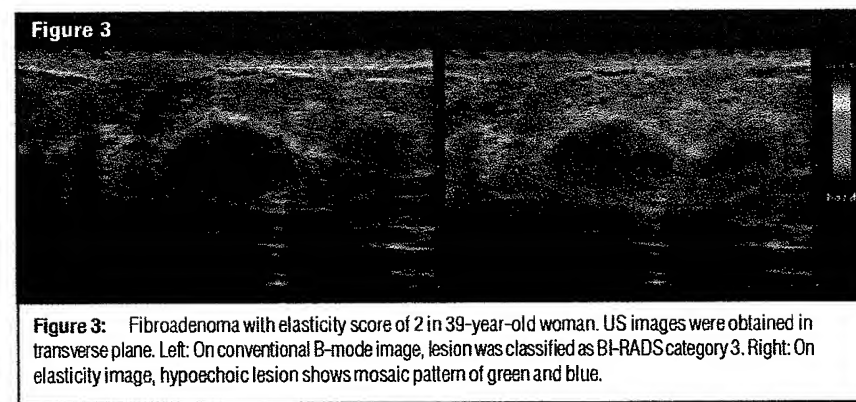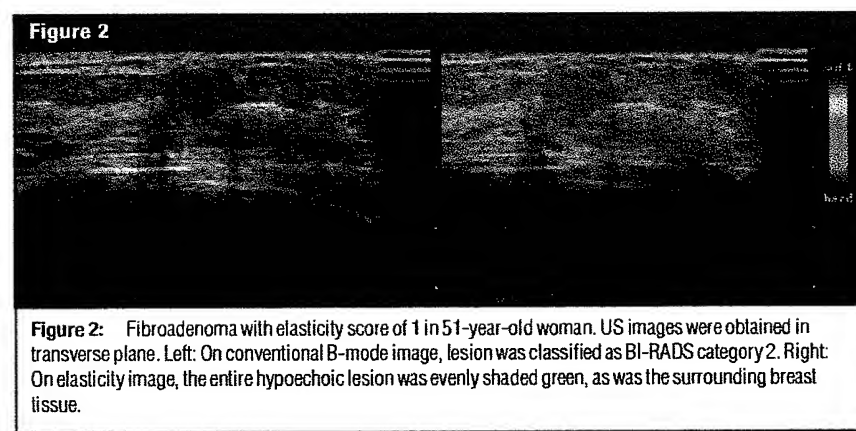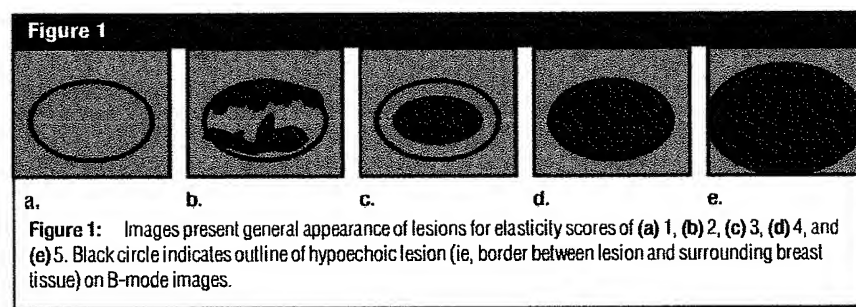
In terms of the ROI used for obtaining elasticity images, we set the top of the

ROI to include subcutaneous fat and the bottom of the ROI to include a pectoral muscle; lateral borders were set more than 5 mm from the lesion's boundary. The ROI needed to be set to include sufficient surrounding breast tissue because elasticity in this system is displayed relative to the average strain inside the ROI. Ideally, elasticity images are obtained by comparing two images—that is, the one obtained before and the one obtained after compression (described later in more detail). In clinical use, however, multiple frames are acquired, and many elasticity images are generated by comparing two adjacent frames during compression and relaxation by continuously moving the probe. The displacement of these two adjacent frames is usually small (< 0.5 mm). In addition, the process of detecting strain was equivalent to the compensation of the displacement. Consequently, elasticity images were produced by comparing an almost identical area on the two images.

The echo signals acquired by using the US scanner were captured by the external computer and were used to calculate of tissue strain with the CAM. First, the amount of tissue displacement induced by compression was calculated with a two-step process. The first step was the rough estimation of displacement by using the correlation of the envelope (ie, the amplitude) of the radio-frequency signals obtained before and after compression. The purpose of this first step was to avoid the error of aliasing and to determine the approximate displacement in the resolution of the half wavelength.

The second step was the fine estimation of displacement, which precisely determined the displacement from the phase difference of the two echo signals before and after compression. Although the second step resembled that of the Doppler US method, the CAM ensured that aliasing errors did not occur because, as a result of the first step, the difference between the true and estimated displacement was reduced to within a half wavelength. Thus, we were able to obtain a fine estimation of displacement without aliasing error.

Next, strain distribution was ob-

Figure 1: Images present general appearance of lesions for elasticity scores of (a) 1, (b) 2, (c) 3, (d) 4, and (e) 5. Black circle indicates outline of hypoechoic lesion (ie, border between lesion and surrounding breast tissue) on B-mode images.

Figure 2: Fibroadenoma with elasticity score of 1 in 51-year-old woman. US images were obtained in transverse plane. Left: On conventional B-mode image, lesion was classified as BI-RADS category 2. Right: On elasticity image, the entire hypoechoic lesion was evenly shaded green, as was the surrounding breast tissue.

Figure 3: Fibroadenoma with elasticity score of 2 in 39-year-old woman. US images were obtained in transverse plane. Left: On conventional B-mode image, lesion was classified as BI-RADS category 3. Right: On elasticity image, hypoechoic lesion shows mosaic pattern of green and blue.

tained from the spatial differentiation of the displacement distribution. The strain distribution was then reconstructed as an elasticity image and was displayed on the computer monitor. The program that was used for this reconstruction was developed at the University of Tsukuba (T.S.) (2–4).

Each pixel of the elasticity image was assigned one of 256 specific colors, depending on the magnitude of strain. The scale ranged from red for components with greatest strain (ie, softest components) to blue for those with no strain (ie, hardest components). Green indicated average strain in the ROI. These color-scale elasticity images were converted to translucent images and were superimposed on the corresponding B-mode images so that the investigator could easily recognize the relationship between strain distribution and the lesion on B-mode images at a glance. Color images were constructed automatically with the same image processing settings throughout the study. Image construction was performed by using a program developed by Hitachi Medical (T.M.) (9).

To obtain a still image for diagnosis, we replayed the recorded motion images and selected an image obtained in the early phase of compression because these images provided the best contrast. Normal breast tissue was displayed in the green range.

To classify elasticity images, we evaluated the color pattern both in the hypoechoic lesion (ie, the area that was hypoechoic or isoechoic relative to the subcutaneous fat [except for echogenic halo] on B-mode images) and in the surrounding breast tissue. On the basis of the overall pattern, we assigned each image an elasticity score on a five-point scale (Fig 1). A score of 1 indicated even strain for the entire hypoechoic lesion (ie, the entire lesion was evenly shaded in green) (Fig 2). A score of 2 indicated strain in most of the hypoechoic lesion, with some areas of no strain (ie, the hypoechoic lesion had a mosaic pattern of green and blue) (Fig 3). A score of 3 indicated strain at the periphery of the hypoechoic lesion, with sparing of the center of the lesion (ie, the peripheral
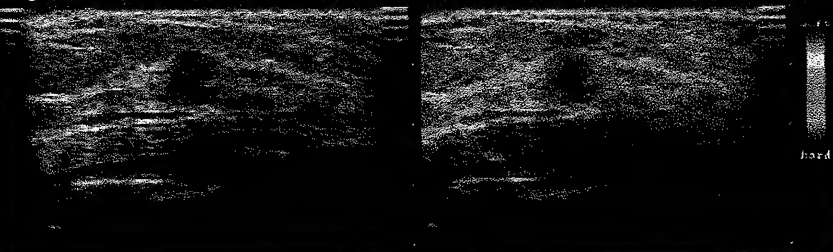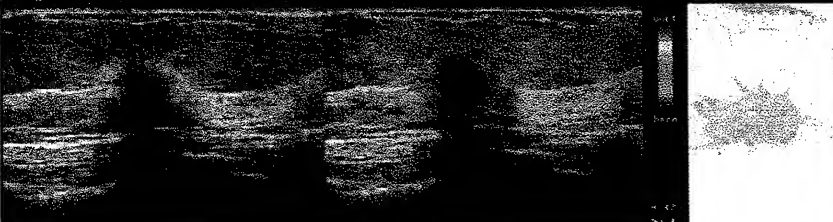

Figure 4:   Lobular carcinoma in situ with elasticity score of 3 in 46-year-old woman. US images were obtained in transverse plane. Left: On conventional B-mode image, lesion was classified as BI-RADS category 3. Right: On elasticity image, the central part of the hypoechoic lesion was blue, and the peripheral part of the lesion was green.
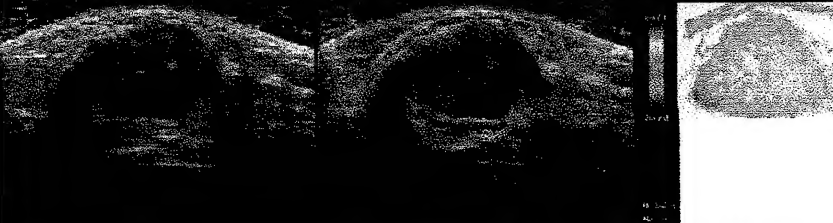
Figure 5:   Nonscirrhous type invasive ductal carcinoma with elasticity score of 4 in 29-year-old woman. US images were obtained in transverse plane. Left: On conventional B-mode image, lesion was classified as BI-RADS category 5. Middle: On elasticity image, the entire hypoechoic lesion was blue. Right: Pathologic section of lesion is shown. (Hematoxylin-eosin stain; original magnification, ×1.)

Figure 6:   Scirrhous type invasive ductal carcinoma with elasticity score of 5 in 55-year-old woman. US images were obtained in sagittal plane. Left: On conventional B-mode image, lesion was classified as BI-RADS category 5. Middle: On elasticity image, both the entire hypoechoic lesion and its surrounding area were blue. Right: Pathologic section of lesion is shown. (Hematoxylin-eosin stain; original magnification, ×1.)

part of lesion was green, and the central part was blue) (Fig 4). A score of 4 indicated no strain in the entire hypoechoic lesion (ie, the entire lesion was

blue, but its surrounding area was not included) (Fig 5). A score of 5 indicated no strain in the entire hypoechoic lesion or in the surrounding area (ie, both the

entire hypoechoic lesion and its surrounding area were blue) (Fig 6).

Scoring was performed by a surgeon (A.I.) who had 5 years of experience in evaluating breast US results according to the imaging patterns described (Fig 1). In the first stage of the study (from March 2002 to March 2003), scoring was performed in 57 lesions, with

knowledge of the results of conventional US examination and the final pathologic diagnosis. In the second stage of the study (from April 2003 to September 2003), scoring was performed in 54 lesions, with knowledge of the results of physical examination and mammography but without knowledge of the results of conventional US examination and the final pathologic diagnosis.

Statistical Analysis

We first compared malignant and benign lesions by (a) comparing the mean elasticity scores for real-time US elasticity images between malignant and benign lesions to determine the score for differentiating between these lesions and (b) comparing the elasticity scores between the three groups within each lesion size category (ie, 4–10 mm, 11–20 mm, and 21–30 mm) to assess the usefulness of this modality for various lesion sizes. All comparisons were made by using the Student t test.

Furthermore, we compared elasticity scores among the histologic subgroups of lesions by using an analysis of variance (Tukey-type multiple comparison) to assess the correspondence between the elasticity score and the compressibility of each histologic type, with pathologic diagnoses as a reference standard.

Finally, we evaluated the ability of the two imaging modalities to allow differentiation of malignant and benign lesions by using a receiver operating characteristic analysis to compare the area under the curve, sensitivity, specificity, and accuracy. Here, the standard proportion test was conducted for sensitivity, specificity, and accuracy. For the indices that did not show a statistically significant difference, we examined equivalence or noninferiority by using the Δ-equivalent test (10).

In addition, we used the χ^2 test to assess the presence of a significant difference between lesions scored in the first stage of the study and those scored in the second stage of the study; as previously noted, the conditions under which scoring was performed were somewhat different.

All statistical tests were performed by using commercially available software (Stat Mate 2000, version 3.01, ATMS, Tokyo, Japan and PASS 2002, NCSS, Kaysville, Utah). For all tests, a P value of less than .05 was considered to indicate a statistically significant difference.

Results

Pathologic Diagnoses

Final pathologic diagnoses are shown in Table 2. All breast cancers were diagnosed histologically by means of radical surgery, excisional biopsy, or needle biopsy. Of the 59 benign lesions, 18 were diagnosed at excisional biopsy, 19 at US-guided needle biopsy, and 22 at fine-needle aspiration cytology. Furthermore, all benign lesions remained unchanged during the follow-up period, which spanned more than 1 year.

Elasticity Scores

The distributions of elasticity scores for malignant lesions and benign lesions are shown in Figures 7 and 8, respectively. The mean elasticity score was significantly higher for malignant lesions (4.2 ± 0.9) than for benign lesions (2.1 ± 1.0) ($P < .001$).

Of the 52 malignant lesions, 45 (86%) lesions, including invasive ductal

Table 2

Final Pathologic Diagnosis in 111 Breast Lesions

Pathologic Diagnosis	No. of Lesions
Malignant lesions	52 (46.8)
Invasive ductal carcinoma	
Nonscirrhous	32 (28.8)
Scirrhous*	10 (9.0)
Ductal carcinoma in situ	9 (8.1)
Mucinous carcinoma	1 (0.9)
Benign lesions	59 (53.2)
ANDI†	24 (21.6)
Fibroadenoma	16 (14.4)
Intraductal papilloma	13 (11.7)
Complex cyst	2 (1.8)
Benign phyllodes tumor‡	2 (1.8)
Lobular carcinoma in situ	1 (0.9)
Granuloma	1 (0.9)

Note.—Numbers in parentheses are percentages.

* Defined as carcinoma that had a hard consistency because of excessive production of dense connective tissue.

† Indicates ANDI without fibroadenoma.

‡ Excisional biopsy was performed in both phyllodes tumors; tumors were proven with histologic analysis.
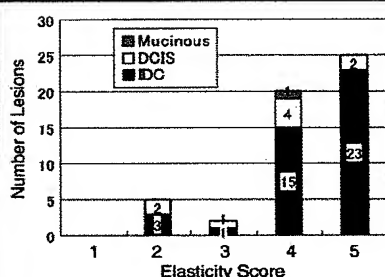
Figure 7

Figure 7: Bar graph demonstrates distribution of elasticity scores for malignant lesions. Numbers on bars indicate the number of lesions. *IDC* = invasive ductal carcinoma, *Mucinous* = mucinous carcinoma.
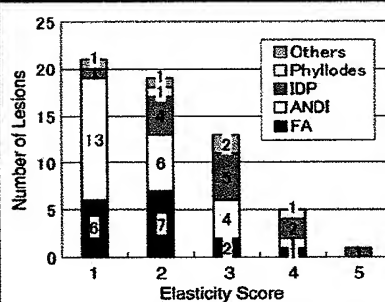
Figure 8

Figure 8: Bar graph demonstrates distribution of elasticity scores for benign lesions. Numbers on bars indicate the number of lesions. For the category termed *others*, lesions included complex cysts, lobular carcinoma in situ, and granulomas. *FA* = fibroadenoma, *IDP* = intraductal papilloma, *Phyllodes* = benign phyllodes tumor.

carcinoma, had a score of 4 or 5. None of the lesions in this group had a score of 1. Of the 59 benign lesions, 40 (68%) lesions, including fibroadenomas and ANDI without fibroadenoma, had a score of 1 or 2 (score of 1, 21 lesions; score of 2, 19 lesions).

One (4%) of the 26 lesions with a score of 5 and five (20%) of the 25 lesions with a score of 4 were benign. Two (13%) of 15 lesions with a score of 3 and five (21%) of 24 lesions with a score of 2 were malignant. Of note, three of the malignant lesions with a score of 2 occurred in the first stage of our study.

The mean elasticity scores according to lesion size on B-mode images are shown in Table 3. For each lesion size category, the mean score was significantly higher for malignant lesions than for benign lesions ($P < .001$).

The distribution of elasticity scores for breast cancers according to their histologic subclassification is shown in Figure 9. The mean score was 3.7 ± 1.0 for DCIS, 4.2 ± 0.9 for invasive ductal carcinoma of nonscirrhous type, and 4.9 ± 0.3 for invasive ductal carcinoma of scirrhous type. There were no significant differences between the mean scores for invasive ductal carcinomas of scirrhous type and those for invasive ductal carcinomas of nonscirrhous type. The mean scores for nonscirrhous carcinoma and those for DCIS did not differ significantly. Mean scores for scirrhous carcinoma and those for DCIS, however, did differ significantly ($P < .05$). Of the five malignant lesions with a score of 2, two were DCIS and three were invasive ductal carcinomas of nonscirrhous type.

The distribution of elasticity scores for benign lesions according to their histologic characteristics is shown in Figure 10. The mean score was 1.9 ± 0.9 for fibroadenoma, 1.7 ± 0.9 for ANDI, and 2.9 ± 1.0 for intraductal papilloma. The mean scores for intraductal papilloma and those for ANDI differed significantly ($P < .01$). In contrast, there was no significant difference between the mean scores for fibroadenoma and those for ANDI or between the mean

scores for intraductal papilloma and those for fibroadenoma.

There was no significant difference between the mean elasticity scores for intraductal papilloma and those for DCIS. However, the mean scores for other benign lesions (fibroadenoma and ANDI) and those for all subclasses of carcinomas differed significantly ($P < .001$ for each comparison).

Diagnostic Performance

Figure 11 shows the receiver operating characteristic curves for elastography and conventional US in differentiating malignant from benign legions. This bar graph shows that the maximum value of the sum of sensitivity and specificity for elastography is higher than that for conventional US. The area under the curve

Table 3

Mean Elasticity Score according to Lesion Diameter

Diameter (mm)*	Malignant	Benign	P Value†
4–10	3.9 ± 1.7 (9)	1.9 ± 0.9 (28)	<.001
11–20	4.4 ± 0.8 (27)	2.3 ± 1.2 (26)	<.001
21–30	4.2 ± 1.0 (16)	2.4 ± 0.6 (5)	<.001

Note.—Elasticity scores are presented as the mean ± standard deviation. Numbers in parentheses indicate the total number of lesions for each size category.

* Lesion diameter was determined at B-mode US and was measured to the nearest millimeter.

† Within each size category, the difference between elasticity scores for malignant and benign lesions was determined to be significant by using the Student t test
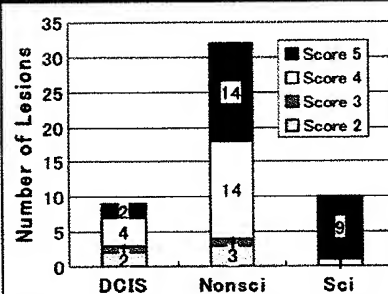

Figure 9: Bar graph demonstrates distribution of elasticity scores for breast cancers according to histologic subclassification. Numbers on bars indicate the number of lesions. *Nonsci* = invasive ductal carcinoma of nonscirrhous type, *Sci* = invasive ductal carcinoma of scirrhous type.
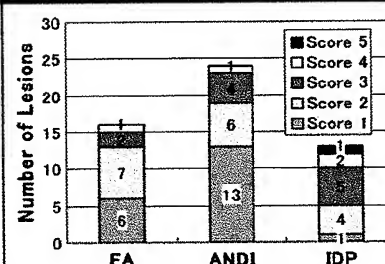

Figure 10: Bar graph demonstrates distribution of elasticity scores for benign lesions according to histologic subclassification. Numbers on bars indicate the number of lesions. *FA* = fibroadenoma, *IDP* = intraductal papilloma.
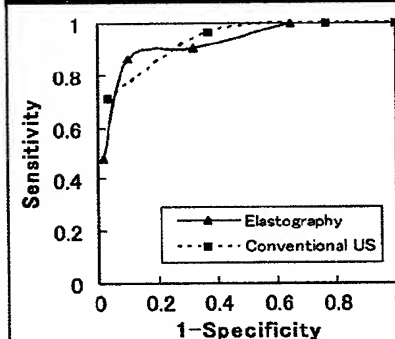

Figure 11: Receiver operating characteristic curves for elastography and conventional US. The area under the curve was almost the same for both elastography and conventional US (0.9185 and 0.9153, respectively). Statistical comparison was not possible because the number of lesions was insufficient.

for elastography was 0.9185, which is slightly higher than that for conventional US (0.9153).

The diagnostic performance of conventional US and of elastography at various cutoff points for the entire study period (stage one and stage two) is shown in Table 4. For elastography, sensitivity (86.5% [45 of 52]; 95% confidence interval: 77.3%, 83.5%), specificity (89.8% [53 of 59]; 95% confidence interval: 82.1%, 97.5%), and accuracy (88.3% [98 of 111]; 95% confidence interval: 82.3%, 94.3%) are shown, with the best cutoff point between elasticity scores of 3 and 4. According to the conventional method, a cutoff point is defined as best if it attains the maximum of value of sum of sensitivity and specificity. The sensitivity (71.2% [37 of 52]; 95% confidence interval: 58.8%, 83.5%), specificity (96.6% [57 of 59]; 95% confidence interval: 92.0%, 100.0%), and accuracy (84.7% [94 of 111]; 95% confidence interval: 78.0%, 91.4%) of conventional US are also shown in Table 4, with the best cutoff point between BI-RADS category 4 and 5. If another cutoff point is applied between BI-RADS category 3 and 4, then sensitivity moves to 96.2% (50 of 52), specificity to 62.7% (37 of 59), and accuracy to 78.4% (87 of 111).

By applying the best cutoff point for each image, we found that elastography had a higher sensitivity than conventional US (P < .05). Elastography had

lower specificity and lower accuracy than conventional US, but these differences were not significant. Therefore, when we considered the equivalence band, the specificity of elastography was not inferior to (ie, not more than 15% different than) (P < .05) and accuracy was equivalent to (ie, within 13% of) (P < .05) that of conventional US.

When the conventional US cutoff point was set between BI-RADS category 3 and 4, only two lesions had false-negative results, but 22 lesions had false-positive results. More than half of the false-positive lesions (14 [64%] of 22 lesions) had elasticity scores of 1 or 2 (score of 1, nine lesions; score of 2, five lesions). When the conventional US cutoff point was set between BI-RADS category 4 and 5, only two lesions had false-positive results, but 15 lesions had false-negative results. More than half of the false-negative lesions (11 [73%] of 15 lesions) had elasticity scores of 4 or 5 (score of 4, eight lesions; score of 5, three lesions).

In contrast, when the cutoff point for elastography was set between scores of 3 and 4, the majority of the false-negative results at elastography (six [86%] of seven lesions) were for lesions with a BI-RADS category of 4 or 5 (category 4, three lesions; category 5, three lesions); the one remaining lesion was classified as BI-RADS category 3. Of the six false-positive findings at elastogra-

phy, three were for BI-RADS category 4 lesions, one was for a BI-RADS category 3 lesion, and two were for BI-RADS category 2 lesions.

In the first stage of the study, the sensitivity, specificity, and accuracy of elastography were 89.3% (25 of 28), 93.1% (27 of 29), and 91.2% (52 of 57), respectively, with a cutoff point of between 3 and 4. Also in the first stage of the study, the sensitivity, specificity, and accuracy of conventional US were 78.6% (22 of 28), 93.1% (27 of 29), and 86.0% (49 of 57), respectively, with a cutoff point of between 4 and 5.

In the second stage of the study, the sensitivity, specificity, and accuracy of elastography were 83.3% (20 of 24), 86.7% (26 of 30), and 85.2% (46 of 54), respectively, with a cutoff point of between 3 and 4. For conventional US, the sensitivity, specificity, and accuracy were 62.5% (15 of 24), 100% (30 of 30), and 83.3% (45 of 54), respectively, with a cutoff point of between 4 and 5. There was no significant difference between the first and second stage of the study with respect to the sensitivity, specificity, and accuracy of elastography and conventional US (P > .05). Therefore, we combined results for the two stages of subsequent analyses.

Discussion

Investigators have performed freehand US elastography in patients with breast lesions by using off-line assessment and have compared the traced outlines of tumors on B-mode images with those on grayscale elastograms (11,12). Although our method is similar to theirs, we were able to make an elasticity assessment instantly because our scoring system was simple; as a result, we believe our system is more practical for clinical use. A freehand US elastography system that permits real-time assessment has been developed and clinically tested. The freehand system uses spatial correlation and has rapid signal processing (12); however, the CAM provides a higher frame rate while maintaining high image quality. The other system uses a one-dimensional search; as a result, the performance of this sys-

---

Table 4

Sensitivity, Specificity, and Accuracy of Elastography and Conventional US at Various Cutoff Points for the Diagnosis of Benign and Malignant Lesions

Cutoff Point*	Sensitivity (%)	Specificity (%)	Accuracy (%)
Elasticity score			
Between 1 and 2	100 (52/52)	35.6 (21/59)	65.8 (73/111)
Between 2 and 3	90.4 (47/52)	67.8 (40/59)	78.4 (87/111)
Between 3 and 4	86.5 (45/52)	89.8 (53/59)	88.3 (98/111)
Between 4 and 5	48.1 (25/52)	98.3 (58/59)	74.8 (83/111)
Conventional US category†			
Between 1 and 2	100 (52/52)	0 (0/59)	46.8 (52/111)
Between 2 and 3	100 (52/52)	23.7 (14/59)	59.5 (66/111)
Between 3 and 4	96.2 (50/52)	62.7 (37/59)	78.4 (87/111)
Between 4 and 5	71.2 (37/52)	96.6 (57/59)	84.7 (94/111)

Note.—Numbers in parentheses were used to calculate percentages.
* Cutoff points are presented for the entire study period (ie, for stage one and stage two).
† Conventional US category was defined according to the BI-RADS classification for US.

tem can be compromised by lateral movement of the probe (11).

From a diagnostic point of view, our findings concur with those of other studies—namely, that elastography is useful for characterizing breast lesions in general and has the potential to allow differentiation between malignant and benign lesions (1,11–13). In the clinical setting, grayscale US elastography during which patients are imaged in a seated position has been performed for those with breast lesions, and motor-driven compression plates have been used (1). Investigators have reported that elastography allowed differentiation of cancers from fibroadenomas, and that the width of the cancers was greater on elasticity images than on B-mode images. Our results, which are derived with the more clinically practical freehand approach, correspond with theirs. In addition, we believe that our system is more rapid for demonstrating longitudinal displacement and more robust for lateral movement of the probe. With our system, lesions can be easily found because translucent color-scale elasticity images are superimposed on the corresponding B-mode images.

Clinical Implications

Although we are not yet able to precisely quantitate elasticity, we have arrived at a point where semiquantitative assessment in the clinical setting is possible.

Our finding of a significant difference between mean elasticity scores for malignant and benign lesions in patients suggests that elastography may be useful in diagnosing breast lesions in the clinical setting. Moreover, this discriminatory capability did not depend on lesion size when lesions were smaller than 30 mm in diameter. The mean elasticity score for scirrhous carcinoma was significantly higher than that for DCIS, and the mean scores for fibroadenoma and ANDI were lower than those for carcinomas. These results agree with experimental results for elastic moduli, as measured in vitro (14).

We believe that an elasticity score of 5, which shows no strain in the entire hypoechoic lesion and the surrounding

area at B-mode US, indicates infiltration of cancer cells into the interstitial tissues (eg, in scirrhous carcinomas) or into an intraductal component (eg, in DCIS), both of which are characteristics of carcinoma.

An elasticity score of 4, which indicates no strain in the entire hypoechoic lesion, seems to be characteristic of tumors such as solid tubular carcinomas that are circumscribed and homogeneously harder than the adjacent normal breast tissue.

In our study, an elasticity score of 3, which indicates strain at the periphery of the hypoechoic lesion, was mainly found in benign lesions, including intraductal papillomas. The importance of strain at the periphery is unclear at present and requires further investigation. We recommend that all lesions with elasticity scores of 3 or higher be examined by means of aspiration cytology or needle biopsy because two (13%) of the 15 lesions with a score of 3 were malignant.

We believe that elasticity scores of 2, for which parts of the hypoechoic lesion did not show strain at B-mode US, indicate lesions that are soft yet somewhat harder than normal breast tissue. This is often characteristic of lesions such as fibroadenoma or ANDI. Of the five malignant lesions with scores of 2, two were DCIS and three were invasive ductal carcinomas at histologic analysis. Investigators have noted that DCIS is softer than invasive ductal carcinoma (14). The finding of a lower elasticity score in lesions suspicious for DCIS is therefore plausible and suggests that correct diagnosis of these lesions will require the use of other imaging modalities in addition to elastography.

Three patients with invasive ductal carcinoma had lesions with a score of 2, but we found no specific histologic features to explain the lower elasticity score in these patients. These false-negative results may have resulted from an artifact that was created by applying the probe with too much pressure during elastography. Two of these lesions were examined in the first stage of our study, and the examiner did not grasp the probe with an appropriate level of pres-

sure. All of the invasive ductal carcinomas with a score of 2 (three lesions) were classified as BI-RADS category 4 or 5, a finding that supports the combined use of elastography and conventional US to avoid misdiagnosing an invasive carcinoma as a benign lesion.

We believe that an elasticity score of 1, which shows even strain in the entire hypoechoic lesion at B-mode US, indicates that lesions have almost the same compressibility as the surrounding breast tissue. In our study, no malignant lesions had a score of 1. Although our findings will require confirmation, this result suggests that invasive diagnostic procedures, such as histologic examination, may be omitted for patients who have lesions with a score of 1.

The result of our receiver operating characteristic curve analysis suggests that elastography may have a diagnostic performance that is better than, or at least equal to, that of conventional US, with the best cutoff point in the means of high sensitivity. Both accuracies coincide with each other within a 13% difference, and the specificity of elastography was not inferior to (ie, not more than 15% different than) that of conventional US. These results show that, compared with conventional US, elastography has higher sensitivity, a noninferior specificity of no more than 15%, and an equivalent accuracy of within 13%, which encourages us to believe that the results were obtained with elastography only. Because classifying elasticity images with our scoring system is simpler than classifying images with a scoring system based on the BI-RADS criteria for conventional US, we believe that even an examiner with limited training may be able to obtain the same diagnostic performance as an experienced examiner with elastography.

Of particular note, 14 (64%) of 22 patients who had false-positive results and a conventional US cutoff point of between BI-RADS category 3 and 4 had elasticity scores of 1 or 2; at minimum, the nine patients with a score of 1 could have conceivably been spared further procedures. In addition, we believe that, with concomitant use of elastogra-

Radiology

phy and conventional US, it may be possible to downgrade some BI-RADS category 3 and 4 lesions to BI-RADS category 2 lesions. As a result, this approach may reduce the number of false-positive results and unnecessary invasive diagnostic procedures.

Limitations

Our study has some limitations. Patients with cancer were overrepresented because our hospital serves as a referral center for general clinics. Therefore, the findings cannot necessarily be extended to the general population. In addition, the lesions that were assessed were predominantly larger lesions. Although elastography facilitated the differentiation of malignant lesions from benign lesions (even among lesions smaller than 10 mm), few lesions in this study were smaller than 5 mm. Therefore, further studies on the use of elastography for the characterization of small lesions will be necessary.

Elastography itself, like all imaging modalities, has certain limitations. The main pitfall of this modality is that the extent of tissue compression influences both the elasticity image and, consequently, the elasticity score. When elasticity scores are used for diagnosis, images obtained with the application of strong pressure may lead to misdiagnosis. Images with minimal perturbation of strain relationships can be obtained by lightly pressing the probe to the breast. It takes some practice to be able to exert light pressure on the same cross-sectional surface of the breast. Of note, three (60%) of five false-negative results obtained by using an elasticity score cutoff point of between 3 and 4 occurred during the first stage of our study when the examiner was just getting used to the probe operation. We cannot, however, determine if the pressure was inappropriate because there is currently no pressure indicator available. Until a pressure gauge becomes available, examiners must attempt to

apply the probe with light pressure by monitoring the real-time image to obtain images that are appropriate for elasticity analysis. Another shortcoming is that, although most images clearly resemble one of the five distinct patterns used for classification, the selection is currently made by the examiner and is not yet automated.

In conclusion, we believe that elastography can complement conventional US, thereby making it easier to diagnose breast lesions. Our experience suggests that the skill needed to acquire adequate images is similar for conventional US and elastography; the skill needed to interpret images, however, is somewhat less for elastography when our classification system is used. Elastography is promising, and we expect that with future improvements in the technology (eg, the development of a pressure indicator and approaches for quantitative assessment), this imaging modality will become an invaluable tool for the diagnosis of breast diseases in the clinical setting.

References
1. Garra BS, Cespedes EI, Ophir J, et al. Elastography of breast lesions: initial clinical results. Radiology 1997;202:79–86.

2. Shiina T, Doyley MM, Bamber JC. Strain imaging using combined RF and envelope autocorrelation processing. In: Proceedings of the IEEE Ultrasonics Symposium. Savoy, Ill: Institute of Electrical and Electronics Engineers Ultrasonics, Ferroelectrics, and Frequency Control Digital Archive, 1996;2: 1331–1336.

3. Shiina T, Nitta N, Ueno E, Bamber JC. Real time tissue elasticity imaging using the combined autocorrelation method. J Med Ultrason 2002;29:119–128.

4. Nitta N, Yamakawa M, Shiina T, Ueno E, Doyley MM, Bamber JC. Tissue elasticity imaging based on combined autocorrelation method and 3-D tissue model. In: Proceedings of the IEEE Ultrasonics Symposium. Savoy, Ill: Institute of Electrical and Electronics

Engineers Ultrasonics, Ferroelectrics, and Frequency Control Digital Archive, 1998;2: 1447–1450.

5. Yamakawa M, Shiina T. Strain estimation using the extended combined autocorrelation method. Jpn J Appl Phys 2001;40:3872–3876.

6. American College of Radiology. Breast imaging reporting and data system (BI-RADS), ultrasound. 4th ed. Reston, Va: American College of Radiology, 2003. Available at: http://www.acr.org/s_acr/sec.asp?CID =882&DID=14550. Accessed September 8, 2004.

7. Japanese Breast Cancer Society. General rules for clinical and pathological recording of breast cancer. 15th ed. Tokyo, Japan: Japanese Breast Cancer Society, 2002.

8. Hughes LE. The ANDI concept and classification of benign breast disorders: an update. Br J Clin Pract Suppl 1989;68:1–6.

9. Matsumura T, Tamano S, Mitake T, et al. Development of freehand ultrasound elasticity imaging system and in vivo results. In: Proceeding of the 1st International Conference on the Ultrasonic Measurement and Imaging of Tissue Elasticity. Rochester, NY: University of Rochester, 2002;1:80.

10. Tango T. Equivalence test and confidence interval for the difference in proportions for the paired-sample design. Stat Med 1998; 17(8):891–908.

11. Hiltawsky KM, Kruger M, Starke C, et al. Freehand ultrasound elastography of breast lesions: clinical results. Ultrasound Med Biol 2001;27:1461–1469.

12. Hall TJ, Zhu Y, Spalding CS. In vivo real-time freehand palpation imaging. Ultrasound Med Biol 2003;29:427–435.

13. Krouskop TA, Younes PS, Srinivasan S, Wheeler T, Ophir J. Differences in the compressive stress-strain response of infiltrating ductal carcinomas with and without lobular features: implications for mammography and elastography. Ultrason Imaging 2003;25: 162–170.

14. Krouskop TA, Wheeler TM, Kallel F, Garra BS, Hall T. Elastic moduli of breast and prostate tissue under compression. Ultrason Imaging 1998;20:260–274.